



Fluorescence resonance energy transfer from pyrene nanoparticles to riboflavin: Spectroscopic insights and analytical application

Dhanshri V. Patil^{a*} & Vishal S. Patil^b

^aDepartment of Chemistry, Krishna Mahavidyalaya, Rethare, Bk-415 108, Maharashtra India

^bDepartment of Chemistry, Sanjeevan Engineering & Technology Institute, Panhala-416 201, Maharashtra India

*E-mail: dtp.phy@gmail.com

Received 28 November 2019; revised and accepted 25 April 2020

The aqueous suspension of fluorescent pyrene nanoparticles (PyNPs) have been prepared by a reprecipitation method in the presence of sodium dodecyl sulphate (SDS) as a stabilizer. The PyNPs shows bathochromically shifted aggregation induced enhanced emission in the spectral region 400 nm to 600 nm peaking at 466 nm where Riboflavin (RF) absorbs strongly. The systematic fluorescence resonance energy transfer (FRET) experiments performed by measuring fluorescence quenching of PyNPs with successive addition of RF analyte has exploited the use of PyNPs as nano probe for detection of RF in aqueous solution with lower limit of detection $10.163 \times 10^{-5} \text{ mol.L}^{-1}$. The fluorescence of PyNPs is quenched by RF and quenching is in accordance with the Stern-Volmer relation. The distance r between the donor (PyNPs) and acceptor (RF) molecules has been obtained according to the FRET method. The evaluation of photo kinetic and thermodynamic parameters such as quenching rate constant (k_q), enthalpy change (ΔH), Gibbs free energy change (ΔG) and entropy change (ΔS) are calculated by quenching results obtained at different constant temperatures. The proposed FRET method based on fluorescence quenching of PyNPs is used further to develop an analytical relation for estimation of RF from pharmaceutical samples available commercially in the market.

Keywords Fluorescent pyrene nanoparticles, Riboflavin, Fluorescence resonance energy transfer

Riboflavin (7, 8-dimethyl-10-ribityl-isoalloxazine) also known as vitamin B₂ is a yellow fluorescent dye, unique among the water soluble vitamins and present in a wide variety of foods. It was firstly isolated from milk and given the name lactochrome. It can be crystallized as orange-yellow crystals^{1,2}. This vitamin is an essential component of two major coenzymes flavin adenine mononucleotide (FMN, also known as riboflavin-5'-phosphate), and flavin adenine dinucleotide (FAD). These coenzymes play major roles in energy production, cellular function, growth, and development, and metabolism of fats, drugs, and steroids³⁻⁵. Various modern investigations strongly recommend that RF has tremendous potential to be used in improving the chemotherapeutic potential of major anticancer drugs⁶. It is very stable during thermal processing, storage and food preparation. It cannot be synthesized in the human body; therefore it must be obtained from dietary sources such as liver, cheese, milk, meat, eggs, wine and tea. Thus, consumption of vitamin B₂ depleted food can result in health problem. RF and related compounds are necessary for cell growth and development. On the

other hand, its concentration in blood must be controlled while most of it is excreted through urine.⁷⁻⁹ The absorption spectrum of RF shows two bands peaking at 372 nm and 445 nm and is known for its characteristic fluorescence¹⁰.

Fluorescence resonance energy transfer (FRET) is a non-radiative process whereby an excited state donor (D) transfers energy to a ground state acceptor (A). The donor and acceptor molecules are coupled by a dipole-dipole interaction. There is no intermediate photon in FRET, and it mainly occurs over distances comparable to most biological macromolecules, i.e., about 10–100 Å^{2,11-12}. Organic probes based on fluorescence quenching approach are widely used for detection and sensing of molecules of physicochemical, biological and environmental concern¹³⁻¹⁴. Perylene, anthracene and pyrene are the most extensively used probes in micellar medium because of their high fluorescence quantum efficiency to sense biomolecules¹⁵, pharmaceutical samples¹⁶, dyes¹⁷, and metal ions¹⁸. On the other hand, the use of aggregation-induced enhanced emission of nanoparticle suspension is of current research interest^{19,20}. The technique of analysis

is based on FRET from pyrene nanoprobe to analyte (RF) molecule. A simple, sensitive and selective fluorimetric detection method is developed for estimation of RF (vitamin B₂) from pharmaceutical samples.

Materials and Methods

Pyrene (Merck-Schuchart) and Riboflavin (Loba-chemie) were used after purity testing. The purity of the compounds was checked by recording their fluorescence spectra at different excitation wavelengths and comparing the values obtained with those reported in the literature. Sodium dodecyl sulphate (SDS) was from SD Fine Chemicals Ltd. and used to generate micellar medium by dissolving in ultrapure water (Millipore, France). The fluorescence and fluorescence excitation measurements were carried out on a PC-based spectrofluorimeter JASCO, Japan (Model FP-750). The excitation and emission slit widths were fixed at 10 nm. The absorption spectra were recorded on Shimadzu UV-3600 spectrophotometer.

The pyrene nanoparticles were prepared by reprecipitation method. The method involved to prepare dilute solution of pyrene (6.82×10^{-3} mol.L⁻¹) in acetone which yielding the monomer fluorescence when recorded under the appropriate excitation wavelength. The surfactant SDS was used and it is found that the solution below critical micelle concentration yielded PyNPs with narrow size distribution, dispersity and with high photo stability. Therefore, 3.6×10^{-3} mol.L⁻¹ SDS concentration was selected for synthesis of PyNPs. The solution of pyrene in acetone was filled in micro syringe and then purged into aqueous solution of SDS under vigorous stirring. The stirring was carried out for about one hour and further subjected to the ultrasonication for about 30 min so as to prolong the stability. The procedure for preparation of PyNPs and all characterization results were reported in our published article²⁰. The RF solution of (1×10^{-4} mol.L⁻¹) was prepared by dissolving calculated amount directly in water and the prepared PyNPs solution was used as energy donor solution in the experiment. An appropriate quantity of PyNPs (1.4×10^{-4} mol.L⁻¹) was kept constant while RF was varied from 0.0 to 1.8 mL and diluted to 5 mL by using water.

Results and Discussion

Photophysical studies on riboflavin and pyrene nanoparticles

The excitation spectrum of RF (A) shows two bands depicting λ_{\max} at 446 nm and the emission

spectrum (B) is structureless with λ_{\max} at 527 nm shown in Fig. 1. The fluorescence spectrum of PyNPs (spectrum- B, Fig. 2) monitored at excitation wavelength 360 nm is a structureless broad band in the region of 380 nm to 600 nm with maximum emission at 466 nm. In the initial, experiments were performed to search the suitable acceptor to PyNPs for formation of donor-acceptor pair. It is observed that RF exhibits strong absorption/excitation in the region of emission of PyNPs (Fig. 1).

The photophysical studies on RF and PyNPs led us to select the PyNPs as a probe (donor) and RF as energy acceptor. These interactions are resulting into fluorescence quenching of PyNPs and establishes the analytical relation for determination of RF from pharmaceutical samples. Fig. 3 shows that there is an overlap between the fluorescence emission spectrum of PyNPs and excitation spectrum of RF which is basic condition required for efficient FRET.

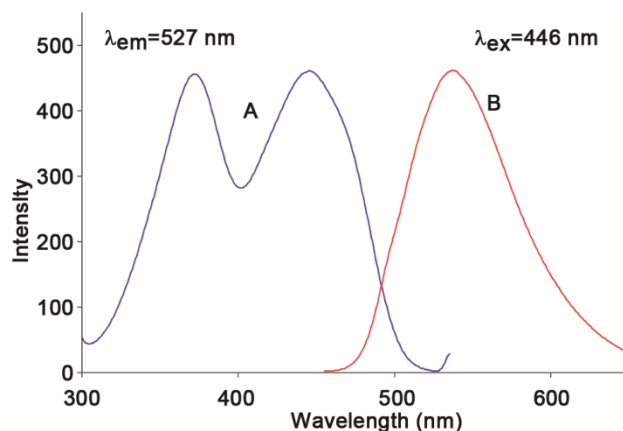


Fig. 1 — The excitation (spectrum-A) and emission (spectrum-B) spectra of RF in aqueous medium.

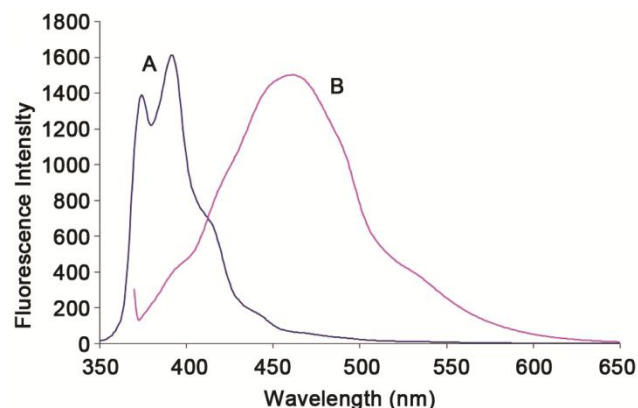


Fig. 2 — Fluorescence spectra of the dilute solution of pyrene in acetone (spectrum-A) and PyNPs in suspension (spectrum-B).

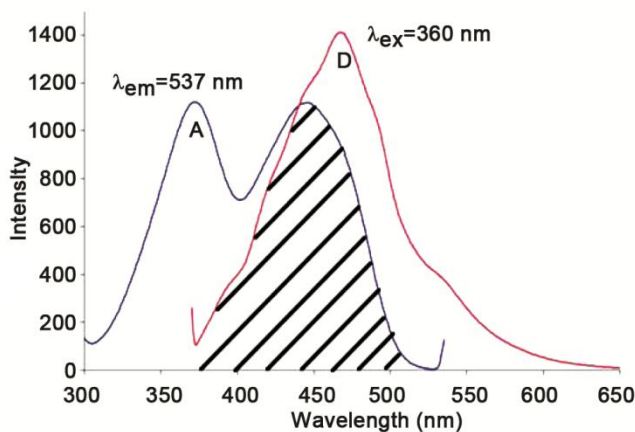


Fig. 3 — Overlap spectra of fluorescence emission of PyNPs (spectrum-D) and excitation of RF (spectrum-A).

UV-visible absorption spectroscopy is very simple and effective method to explore the structural change and to know the complex formation in solution²¹. The results of the UV-visible spectral scans are presented in Fig. 4. The spectrum 'a' and spectrum 'k' are of pure PyNPs and RF, respectively. The PyNPs shows two peaks one at 265 nm due to aromaticity and another broad band in the region 320-500 nm due to strong π - π stacking interactions of the neighboring molecules in the nanoparticles cluster²². RF gives four peaks with maximum absorption at 225 nm, 265 nm, 377 nm and 445 nm. Hence, it is observed that with increasing concentration of RF the absorption intensity also increases without any spectral shift giving idea about the absence of ground-state complex formation and existence of dynamic quenching in present PyNPs-RF system. Dynamic quenching is observed due to diffusion and it affects only the excited state of quenching molecule while it has no effect on the absorption spectrum of the quenching substances².

Fluorescence quenching of PyNPs by excited state interaction with RF

Fluorescence quenching refers to any process that decreases the fluorescence intensity of a probe by molecular interaction²³. The fluorescence spectra of PyNPs in absence and presence of different concentrations of RF scanned in the range 370-650 nm at 305 K temperature are shown in Fig. 5. The spectra reveal that the PyNPs has fluorescence emission band in the region 370-550 nm with λ_{max} at 466 nm when excited at 360 nm. The fluorescence intensity of PyNPs decreases gradually with increase in concentration of RF. The isoemissive point seen clearly at 492 nm indicates excited state equilibrium

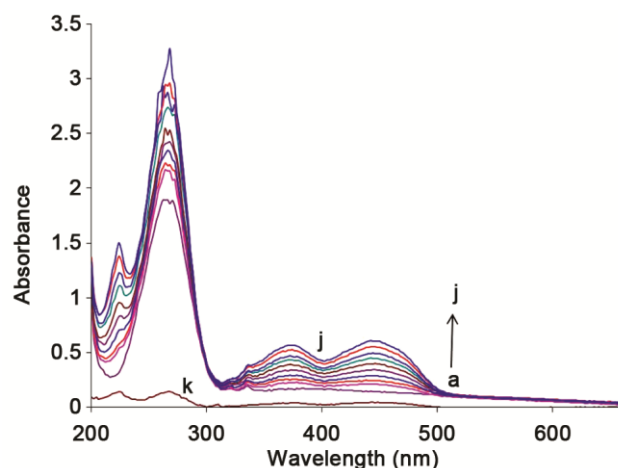


Fig. 4 — Absorption spectra of PyNPs ($6.8 \times 10^{-5} \text{ mol.L}^{-1}$) in absence and presence of different concentrations of RF (spectra from a to j) corresponding to [0.0, 0.4, 0.8, 1.2, 1.6, 2.0, 2.4, 2.8, 3.2, 3.6] $\times 10^{-5} \text{ mol.L}^{-1}$ and spectrum-k is of pure RF at 305 K.

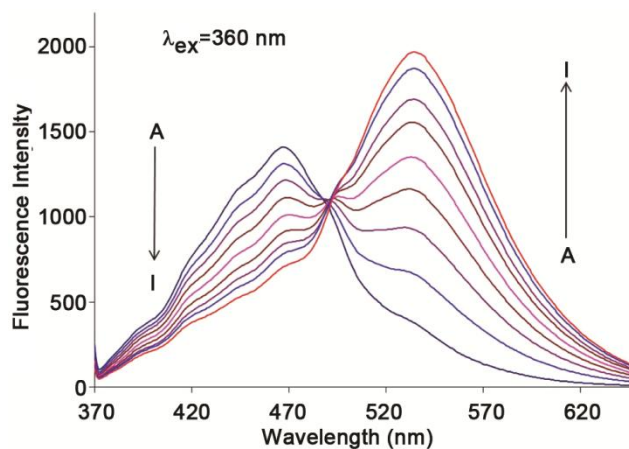


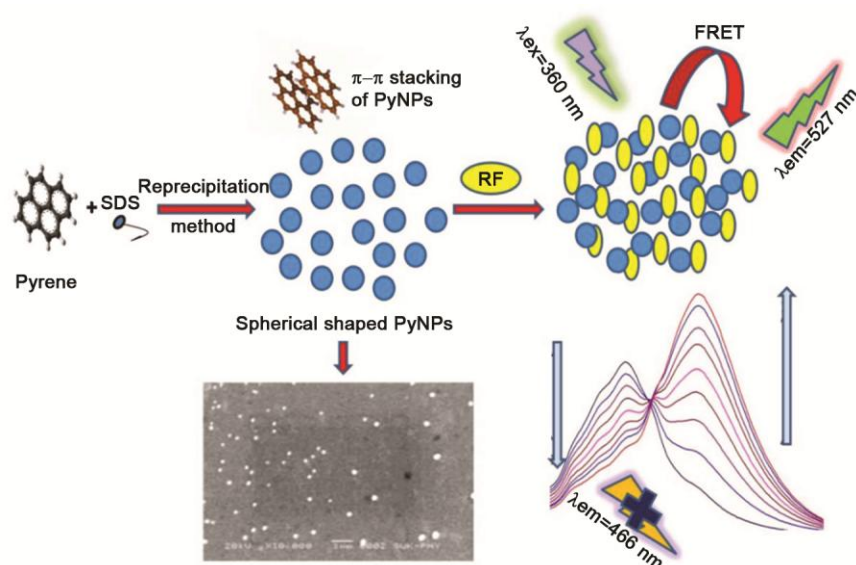
Fig. 5 — The fluorescence quenching spectra of PyNPs, from A to I: [PyNPs] = $6.8 \times 10^{-5} \text{ mol.L}^{-1}$; [RF] = 0.0, 0.4, 0.8, 1.2, 1.6, 2.0, 2.4, 2.8, 3.2, $3.6 \times 10^{-5} \text{ mol.L}^{-1}$ at 305 K.

between two components and the fluorescence resonance energy transfer²⁴. Same set of experiment was repeated at another two different constant temperatures 310 K and 315 K. The quenching of fluorescence may be static or dynamic and can be recognized by temperature dependence studies. The proposed mechanism of FRET from SDS capped PyNPs to RF is shown in Scheme 1.

Stern-Volmer plots

The fluorescence quenching data at three different temperatures (305 K, 310 K and 315 K) were analysed by using Stern-Volmer equation².

$$\frac{F_0}{F} = 1 + K_{sv}[Q] = 1 + k_q\tau_0[Q] \quad \dots (1)$$



Scheme 1 — The proposed mechanism of FRET from SDS capped PyNPs to RF

where F_0 and F are the fluorescence intensities of PyNPs in the absence and presence of quencher RF, respectively, k_q is the quenching rate constant, K_{sv} is the Stern-Volmer dynamic quenching constant, τ_0 is the excited state lifetime of the PyNPs in absence of RF ($\tau_0 = 6.6 \times 10^{-9}$ s) and $[Q]$ is the concentration of quencher i.e. RF. The quenching rate constants are expected to increase with increase in temperature for dynamic quenching while for static quenching reverse effect is observed.

The Stern-Volmer plots for PyNPs-RF system are shown in Fig. 6. The plots are linear with the slopes increasing with increase in temperature. The values of K_{sv} obtained from the slopes of lines at three different temperatures are given in Table 1. The values indicate that the probable mechanism of fluorescence quenching is of dynamic quenching involving interactions between two components. The values of quenching rate constants are calculated from the relation,

$$k_q = K_{sv} / \tau_0 \quad \dots (2)$$

The calculated quenching rate constants, given in Table 1, are increased with temperature and supports conclusion of dynamic quenching in present system²³.

Binding constants and binding sites

The binding of RF to PyNPs was determined by using the following equation¹¹.

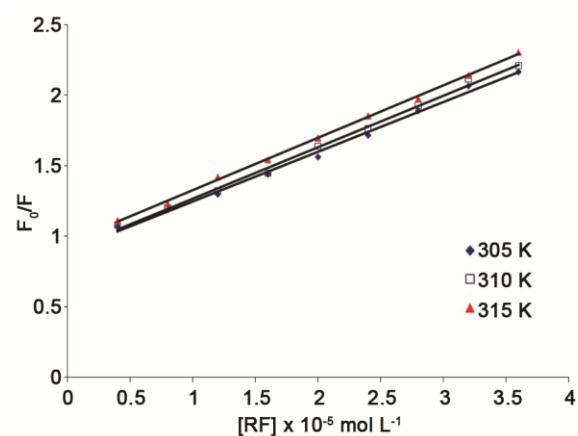


Fig. 6 — The Stern-Volmer plots at three different temperatures

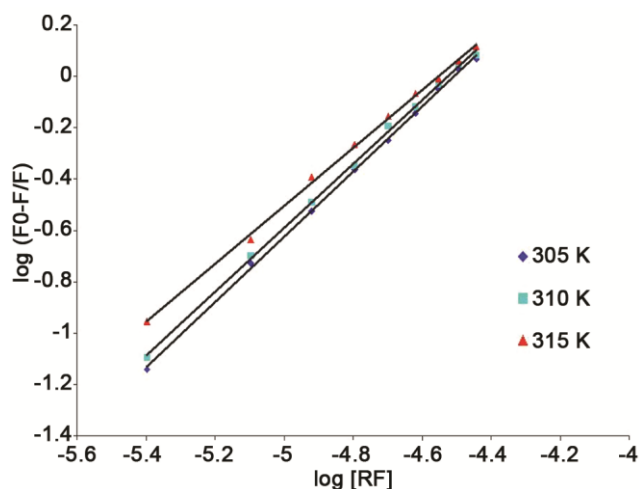
Table 1 — Stern-Volmer quenching constants and quenching rate constants of the PyNPs-RF system at different temperatures

T (K)	K_{sv} (10^4 L.mol ⁻¹)	k_q (10^{12} L.mol ⁻¹ .s ⁻¹)	*R
305	3.533	5.359	0.9971
310	3.658	5.542	0.9983
315	3.727	5.646	0.9986

*R is the correlation coefficient.

$$\log \frac{(F_0 - F)}{F} = \log K + n \log [Q] \quad \dots (3)$$

where K and n are the binding constant and number of binding sites, respectively. The values of K and n were obtained from the plot of $\log (F_0 - F)/F$ versus $\log [RF]$, as shown in Fig. 7. The calculated data for K and n are given in Table 2.

Fig. 7 — Plot of $\log (F_0-F)/F$ vs $\log [RF]$.Table 2 — The binding constants (K) and number of binding sites (n).

T (K)	K (10^5 L.mol^{-1})	n	* R
305	5.276	1.269	0.9995
310	4.182	1.242	0.9994
315	1.3167	1.142	0.9987

* R is the correlation coefficient.

It is observed that the binding constant (K) decreases with rise in temperature as per expectation. The values of n approximately equal to one indicated the existence of only a single binding site on PyNPs. The correlation coefficients are larger than 0.998, indicating that the interaction between PyNPs and RF agrees well with the site binding model based on Eqn 3²⁵.

Thermodynamic parameters and nature of the binding forces

The thermodynamic parameters of binding interaction are the main evidences for confirming the binding force. If the condition where enthalpy changes (ΔH) does not vary significantly over the temperature range of experiments, then its value and that of entropy change (ΔS), free energy change (ΔG) can be determined from the van't Hoff equation.

$$\ln K = -\frac{\Delta H}{RT} + \frac{\Delta S}{R} \quad \dots (4)$$

$$\text{and } \Delta G = \Delta H - T\Delta S \quad \dots (5)$$

where K is the binding constant at corresponding temperature and R is the gas constant²⁶. The enthalpy change (ΔH) and entropy change (ΔS) were obtained from the slope and intercept of the line obtained in van't Hoff plot of $\ln K$ versus $1/T$, shown in Fig. 8.

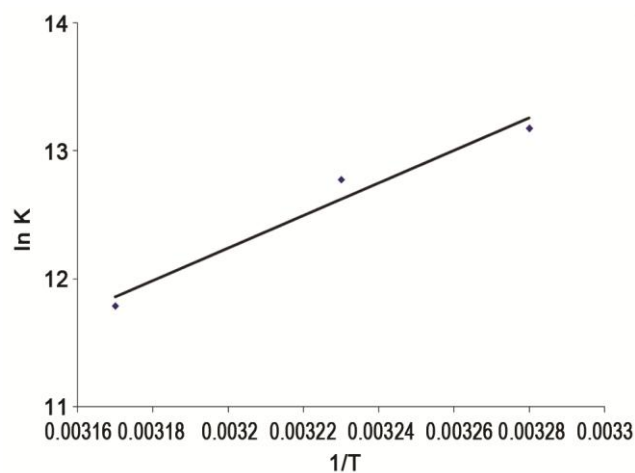


Fig. 8 — van't Hoff plot for binding of RF with PyNPs.

Table 3 — The thermodynamic parameters for the PyNPs-RF FRET system.

T (K)	ΔH (kJ.mol^{-1})	ΔG (kJ.mol^{-1})	ΔS ($\text{J.mol}^{-1}.\text{K}^{-1}$)	* R
305		-33.734		
310	-106.726	-32.538	-239.318	0.9810
315		-31.341		

* R is the correlation coefficient.

The values of thermodynamic parameters i.e. ΔH , ΔS and ΔG are listed in Table 3. The negative values of $\Delta H = -106.726 \text{ kJ.mol}^{-1}$ and $\Delta S = -239.318 \text{ J.mol}^{-1}.\text{K}^{-1}$ indicate that the hydrogen bonding and van der Waal's forces are the major interacting forces. Also, the binding is mainly enthalpy-driven and the entropy is unfavorable for it²⁷. Hydrogen bonds are specific and directed. These are probably best identified through their negative enthalpy formation²⁸. The negative value of ΔG reveals that the interaction process is spontaneous.

Energy transfer between PyNPs and RF

In order to know more details about energy transfer, the efficiency of energy transfer (E) and the interaction distance (r) between donor and acceptor can be calculated by using Förster's theory. This is a non-destructive spectroscopic method that can monitor the proximity and relative angular orientation of fluorophores.

A transfer of energy could take place through direct electro dynamic interaction between the primarily excited molecule and its neighbours²⁹. According to this theory, the binding distance between PyNPs and RF could be calculated by the equation^{30,31}.

$$E = \frac{R_0^6}{R_0^6 + r^6} \quad \dots (6)$$

$$R_0^6 = 8.79 \times 10^{-25} \cdot K^2 \cdot n^{-4} \cdot \phi_d \cdot J \quad \dots (7)$$

$$E = 1 - \frac{F}{F_0} \quad \dots (8)$$

where E denotes the energy transfer efficiency, R_0 is the critical distance at which the transfer efficiency equals to 50% and r is distance between the donor and acceptor pairs. In Eqn (7), K^2 is the spatial orientation factor for the donor and acceptor dipoles and K^2 is usually assumed to be equal to 0.667, which is appropriate for dynamic random averaging of the donor and acceptor positions³². n is the refractive index of the medium, ϕ_d is the fluorescence quantum yield of the donor (PyNPs) in absence of acceptor, J is the spectral overlap integral between the emission spectrum of donor and the excitation spectrum of acceptor. Under these experimental conditions, using $n = 1.336$, $\phi_d = 0.467$ (fluorescence quantum yield of PyNPs calculated based on the reference method with quinine sulphate as the fluorescence standard³³) and $J = 0.4824 \times 10^{-13} \text{ cm}^3 \cdot \text{L} \cdot \text{mol}^{-1}$ the value of $E = 0.3406$ and $R_0 = 40.18 \text{ \AA}$ has been estimated. The value of R_0 less than 50 \AA is an indication of efficient energy transfer between the donor-acceptor pair³⁴. Also, value of $r = 4.48 \text{ nm}$ which ranges in between 2-8 nm scale indicates that the energy transfer from PyNPs to RF occurs with high probability³⁵.

Analysis of RF from pharmaceutical samples

The RF is available in the form of tablets and injections. Therefore, the proposed quenching method was applied for estimation of RF (vitamin B₂) in

pharmaceutical samples namely CoBadex Forte capsule and Polybion injection. For the analysis purpose, both are dissolved separately in ultrapure water and diluted to the required volume by the same solvent. Then, this solution was used for the quenching experiment along with the standard set given in experimental section. The calibration plot for the determination of RF is constructed by plotting F_0/F versus RF concentration as shown in Fig. 9.

The plot depicts a good linear relationship between the fluorescence quenching intensity and concentration of RF, with a correlation coefficient (R) of 0.9921. The corresponding linear regression equation is $y = 0.3306x + 1$ and was used to calculate unknown concentrations of RF from pharmaceutical dissolutions. The results obtained are in good agreement with certified values given in Table 4. The

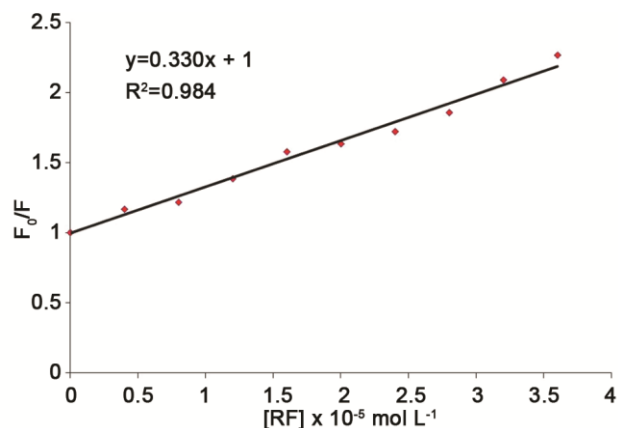


Fig. 9 — Calibration graph for analysis of RF from pharmaceutical samples

Table 4 — Determination of riboflavin in pharmaceutical samples

Sample	Composition	Amount of Riboflavin		RSD (%)
		Certified value	Found*	
Polybion (2 ml) (Injection of vit. B complex with vit. B ₁₂) (Merck limited, Usgaon, Ponda, Goa-403 407)	Thiamine hydrochloride IP 10 mg	4.00 mg (per injection)	3.968 mg (per injection)	1.023
	Riboflavin Sodium Phosphate IP 4 mg			
	Pyridoxine hydrochloride IP 4 mg			
	Nicotinamide IP 40 mg			
	Cyanocobalmin IP 8 µg			
D-Panthenol IP 6 mg				
CoBadex Forte Capsule (GlaxoSmithKline Pharmaceutical Limited)	Thiamine mononitrate IP 10 mg	10.00 mg (per capsule)	9.945 mg (per capsule)	.411
	Vitamin B ₂ IP 10 mg			
	Nicotinc acid IP 100 mg			
	Calcium pantothenate IP 50 mg			
	Vitamin B ₁₂ IP 15 µg			
	Vitamin B ₆ IP 3 mg			
	Vitamin C IP 150 mg			
	Folic acid IP 1500 µg			
	Biotin USP 100 µg			

* Average of five determinations

limit of detection (LOD) of the method was $10.163 \times 10^{-5} \text{ mol.L}^{-1}$, calculated by the equation $\text{LOD} = (3\sigma/k)$, where σ is the standard deviation of the y-intercept of the regression lines and k is the slope of the calibration graph³⁶. Thus, the proposed method is very simple, selective and reproducible for analysis of pharmaceutical samples containing RF.

Conclusions

The molecular interactions between PyNPs and RF are investigated by using fluorescence resonance energy transfer. So, it is conclusively said that they undergo significant interactions in the excited state and weak interactions in ground state. Again, on the basis of Försters energy transfer mechanism, energy transfer parameters have been evaluated. The fluorescence of PyNPs was quenched by RF and proved the validity of Stern-Volmer relation. The temperature dependence study revealed the Stern-Volmer quenching constants and quenching rate constants, both increases with rise in temperature, indicating the dynamic quenching mechanism in present system. The thermodynamic parameters ΔH , ΔS and ΔG at different temperatures were calculated and results indicated that the hydrogen bonds and van der Waal's interactions are the major binding forces. The binding distance $r = 4.48 \text{ nm}$ between PyNPs-RF was obtained according to FRET which indicated high probability of energy transfer. The analytical method is developed and applied successfully to estimate RF directly from pharmaceutical formulations by using quenching mechanism

References

- 1 Powers H J, *Am J Clin Nutr*, 77 (2003) 1352.
- 2 Patil D T, Bhattar S L, Kolekar G B & Patil S R, *J Solution Chem*, 40 (2011) 211.
- 3 Coates P M, Betz J M, Blackman M R, Cragg G M, Levine M, Moss J & White J D Encyclopedia of Dietary Supplements (2nd ed.) London and New York: Informa Healthcare (2010) 691.
- 4 Ross A C, Caballero B H, Cousins R J, Tucker K L & Ziegler T R, *Modern Nutrition in Health and Disease* (11th ed.) Baltimore, M D: Lippincott Williams & Wilkins (2014) 325.
- 5 Washington D C, Institute of Medicine. Food and Nutrition Board *Dietary Reference Intakes: Thiamin, Riboflavin, Niacin, Vitamin B6, Folate, Vitamin B12, Pantothenic Acid, Biotin, and Choline*. National Academy Press (1998).
- 6 Naseem I, Hassan I, Alhazza I M & Chibber S, *J Trace Elem Med Biol*, 29 (2015) 303.
- 7 Silpi D, Mukhopadhyay C & Bose S K, *Bull Chem Soc Jpn*, 76 (2003) 1729.
- 8 Hu L, Yang X, Wang C, Yuan H & Xiao D, *J Chromatogr B*, 856 (2007) 245.
- 9 Roy D K, Deb N, Ghosh B C & Mukherjee A K, *Spectrochim Acta A*, 73 (2009) 201.
- 10 More V R, Mote U S, Patil S R & Kolekar G B, *J Solution Chem*, 39 (2010) 97.
- 11 Patil D T, Mokashi V V, Kolekar G B & Patil S R, *Luminescence*, 28 (2013) 821.
- 12 Tang Z, Liu X, Wang Y, Chen Q, Hammock B D & Xu Y, *Environ Pollut*, 251 (2019) 238.
- 13 Desai V R, Hunagund S M, Basanagouda M, Kadadevarmath J S & Sidarai A H, *J Fluores*, 27 (2017) 1839.
- 14 Patil N R, Melavanki M, Kapatkar S B, Chandrashekhar K, Patil H D & Umapathy S, *Spectrochim Acta A*, 79 (2011) 1985.
- 15 Bhattar S L, Kolekar G B & Patil S R, *J Lumin*, 128 (2008) 306.
- 16 Bhopate D P, Mahajan P G, Garadkar K M, Kolekar G B & Patil S R, *Luminescence*, 30 (2015) 1055.
- 17 Bhattar S L, Kolekar G B & Patil S R, *J Disp Sci Tech*, 32 (2009) 23.
- 18 Backhus D A & Gschwend P M, *Environ Sci Technol*, 24 (1990) 1214.
- 19 Gore A H, Gunjal D B, Kokate M R, Sudarsan V, Anbhule P V, Patil S R & Kolekar G B, *ACS Appl Mater Interfaces*, 4 (2012) 5217.
- 20 Patil D V & Patil V S, *Indian J Chem* 58A (2019) 1187.
- 21 Suryavanshi V D, Anbhule P V, Gore A H, Patil S R & Kolekar G B, *Ind Eng Chem Res*, 51 (2012) 95.
- 22 Zhang X, Zhang X, Shi W, Meng X, Lee C & Lee S, *J Phys Chem B*, 109 (2005) 18777.
- 23 Lakowicz J R, *Principles of Fluorescence spectroscopy*, Springer publication, University of Maryland School of Medicine, Baltimore, USA (2006).
- 24 More V R, Mote U S, Patil S R & G B Kolekar, *Spectrochim Acta A*, 74 (2009) 771.
- 25 Wang Y Q, Tang B P, Zhang H M, Zhou Q H & Zhang G C, *J Photochem Photobiol B*, 94 (2009) 183.
- 26 Zhang G, Chen X, Guo J & Wang J, *J Mol Struct*, 921 (2009) 346.
- 27 Ross P D & Subramanian S, *Biochem*, 20 (1981) 3096.
- 28 Wang F, Huang W, L Su, Z Dong & S Zhang, *J Mol struct*, 927 (2009) 1.
- 29 T. Förster, *Ann Phys*, 2 (1948) 55.
- 30 Clegg R M, *Curr Opin Biotech*, 6 (1995) 103.
- 31 Kumar G A & Unnikrishnan N V, *J Photochem Photobiol*, A 144 (2001) 107.
- 32 Cao S, Wang D, Tan X & Chen J, *J Solution Chem*, 38 (2009) 1193.
- 33 Chen G Z, Huang X Y & Zheng Z Z, *Fluor Anal Methods*, (2nd edition) Science Press, Beijing, (1990) 15.
- 34 Salvatore A, Marras E, Kramer F R & Tyagi S, *Nucl Acid Res*, 30 (2002) 122.
- 35 Hu Y J, Lu Y, Shen X S, Fang X Y & Qu S S, *J Mol Struct*, 738 (2005) 143.
- 36 Patil D V, Patil V S, Sankpal S A, Kolekar G B & Patil S R, *J Inclusion Phenom Macrocyclic Chem*, 90 (2018) 99.